

Distributed Poisson multi-Bernoulli filtering via generalised covariance intersection

Ángel F. García-Fernández, Giorgio Battistelli

Abstract—This paper presents the distributed Poisson multi-Bernoulli (PMB) filter based on the generalised covariance intersection (GCI) fusion rule for distributed multi-object filtering. Since the exact GCI fusion of two PMB densities is intractable, we derive a principled approximation. Specifically, we approximate the power of a PMB density as an unnormalised PMB density, which corresponds to an upper bound of the PMB density. Then, the GCI fusion rule corresponds to the normalised product of two unnormalised PMB densities. We show that the result is a Poisson multi-Bernoulli mixture (PMBM), which can be expressed in closed form. Future prediction and update steps in each filter preserve the PMBM form, which can be projected back to a PMB density before the next fusion step. Experimental results show the benefits of this approach compared to other distributed multi-object filters.

Index Terms—Multi-object filtering, distributed fusion, Poisson multi-Bernoulli, generalised covariance intersection.

I. INTRODUCTION

Multiple object filtering (MOF) aims to determine the unknown and time-varying number of objects and their states based on noisy sensor data. This field has many applications including autonomous vehicles [1], space surveillance [2] and marine traffic monitoring [3]. MOF can be performed by a number of collaborative agents that sense the environment and then fuse their information to obtain a better understanding of the scene [4]. Multi-agent MOF has several advantages over single-agent MOF such as increased robustness, improved performance and the possibility to monitor larger areas [5].

MOF is often addressed using probabilistic inference via random finite sets (RFSs) [6]. In this approach, all information about the current set of objects is contained in the density of the set of objects given all measurements up to the current time step (posterior density). A number of single-agent MOF algorithms that compute or approximate the posterior density under different modelling assumptions have been proposed. For instance, MOF algorithms based on a labelled RFS (which require a multi-Bernoulli birth model with uniquely labelled objects upon birth) are the generalised labelled multi-Bernoulli (GLMB) filter [7] and the labelled multi-Bernoulli (LMB) filter [8]. MOF algorithms based on a Poisson point process (PPP) birth model without object labelling are the probability hypothesis density filter [6], the Poisson multi-Bernoulli

mixture (PMBM) filter [9], [10] and Poisson multi-Bernoulli (PMB) filters [9], [11]. PMBM and PMB filters can also be adapted to multi-Bernoulli birth model [12].

To perform multi-agent MOF, there are two main rules to fuse the information contained in two multi-object densities (without known dependencies) in a principled manner: generalised covariance intersection (GCI) [13] and arithmetic average (AA) [14]. Importantly, both GCI and AA are optimal in the sense of minimising a weighted sum of Kullback-Leibler divergences (KLDs) w.r.t. the fusing densities [14], [15]. For MOF algorithms with labelled objects, the GCI rule has been used for general multi-object densities, GLMB and LMB densities in [16] and also for LMB densities in [17], [18]. The AA fusion rule has been applied to GLMB and LMB densities in [19].

A theoretical challenge with distributed fusion with labelled objects is that the direct application of the GCI and AA fusion rules can be problematic as different agents may have assigned different labels to the same potential object. Distributed labelled RFS algorithms therefore require external procedures to resolve label mismatches before applying the GCI or AA fusion rules. These procedures, such as explicit label-to-label association or relabelling steps [16] [19], are not part of the original GCI/AA formulation, but must be performed beforehand to ensure label consistency across agents. Another strategy to sort out label mismatches in practice is to first remove the labels, perform the fusion and then add them afterwards, for example, as done for GLMB/LMB densities in [20] and in the hybrid LMB and probability hypothesis density (PHD) fusion algorithm in [21]. The label mismatch problem can also complicate the standard use of labels in labelled RFS theory for sequential trajectory estimation, though it is always possible to recover trajectory information from the sequence of filtered densities on the set of unlabelled objects [22].

Fusion of multi-object densities without object labelling is not affected by the theoretical limitation of label mismatches. With the AA rule, distributed AA-PHD filters have been proposed in [15], [23] and a distributed AA-PMBM filter in [24]. With the GCI rule, distributed GCI-PHD filters were proposed in [25]–[28], a distributed GCI Bernoulli filter was proposed in [29], and a distributed multi-Bernoulli filter was proposed in [30]. A fusion rule based on GCI is applied to a PMBM filter for extended objects in [31], but it does not actually perform GCI on the full PMBM as it only fuses single-object density parameters in an ad-hoc manner. In [32], a fusion rule for PMBs based on minimising an upper bound of the GCI-KLD cost function [14] is proposed. This fusion rule requires that the number of Bernoulli and PPP components is

A. F. García-Fernández is with the IPTC, ETSI de Telecomunicación, Universidad Politécnica de Madrid, 28040 Madrid, Spain (email: angel.garcia.fernandez@upm.es).

G. Battistelli is with Dipartimento di Ingegneria dell'Informazione (DINFO), Università di Firenze, Via Santa Marta 3, 50139, Firenze, Italy (e-mail: giorgio.battistelli@unifi.it).

The authors would like to thank the financial support of the Royal Society International Exchanges Award IES\R1\231122.

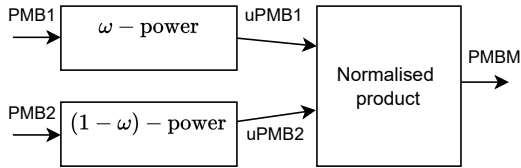


Figure 1: Approximate GCI fusion rule (with parameter $\omega \in [0, 1]$) for two PMB densities. The ω and $1 - \omega$ powers of the PMB densities (PMB1, PMB2) are upper bounded by unnormalised PMB densities (uPMB1, uPMB2). The normalised product of these is a PMBM. The PMBM can then be projected back to a PMB [9], [11].

the same for all agents, which is achieved by dividing the PPP into different PPPs. The fusion rule has a degree of freedom that is the choice of the permutations that assign Bernoulli and PPP components across all agents. These permutations are chosen by minimising a symmetric KLD between the single-object densities of the Bernoulli/PPP components.

The main contribution of this paper is the derivation of a principled mathematical approximation of the GCI fusion rule for two PMB densities, and the resulting distributed MOF algorithms. The only approximation involved is in the computation of the power of a PMB, which we approximate by an unnormalised PMB density with a closed-form expression. This approximation results from approximating the power of a sum by a sum of powers, which is an upper bound and a standard approximation in GCI fusion [26]. Then, the GCI rule consists of the calculation of the normalised product of these unnormalised PMB densities. We show in this paper that this product is a PMBM density with a closed-form expression, see Figure 1 for a diagram. This procedure naturally assigns potential objects in the two densities, with the possibility of leaving them unassigned, without the need of external assignment procedures. We also show that the proposed GCI-PMB fusion rule minimises a lower bound on the GCI weighted sum of KLDs. A second contribution is the Gaussian implementation of the GCI-PMB fusion rule. A third contribution is the extension of the proposed fusion rule to sensors with limited fields of view (FoVs). Simulation results show the benefits of the proposed fusion rule.

The rest of the paper is organised as follows. Section II presents the problem formulation. The approximate GCI fusion rule for two PMBs is derived in Section III. Section IV addresses the Gaussian implementation of the GCI-PMB fusion rule. Section V explains how to extend this fusion rule to sensors with limited FoVs. Lastly, simulation results and conclusions are provided in Sections VI and VII, respectively.

II. PROBLEM FORMULATION

This paper deals with distributed multi-object filtering using PMB filters. In particular, we consider that there are a number of sensors/nodes/agents in the scenario, each independently performing its own PMB filtering. In this context, the aim of this paper is to develop the GCI fusion for two PMB densities. The result can be applied to the information fusion for any number of nodes via sequential fusion [33].

Let $x \in \mathbb{R}^{n_x}$ be a single-object state and X be the set of object states, where $X \in \mathcal{F}(\mathbb{R}^{n_x})$, which denotes the set

of all finite subsets of \mathbb{R}^{n_x} . We consider two nodes, indexed by $s \in \{1, 2\}$. After processing their measurements, node s represents the information on X as a PMB density [9]

$$f_s(X) = \sum_{X^0 \uplus \dots \uplus X^{n_s} = X} f_s^p(X^0) \prod_{i=1}^{n_s} f_s^i(X^i), \quad (1)$$

where the sum goes through all mutually disjoint sets X^0, \dots, X^{n_s} such that their union is X , n_s is the number of Bernoulli components, $f_s^p(\cdot)$ is the PPP density and $f_s^i(\cdot)$ is the i -th Bernoulli density. These densities have the form

$$f_s^p(X) = e^{-\int \lambda_s(x) dx} [\lambda_s]^X \quad (2)$$

$$f_s^i(X) = \begin{cases} 1 - r_s^i & X = \emptyset \\ r_s^i p_s^i(x) & X = \{x\} \\ 0 & \text{otherwise,} \end{cases} \quad (3)$$

where $\lambda_s(\cdot)$ is the PPP intensity, $[\lambda_s]^X = \prod_{x \in X} \lambda_s(x)$, with $[\lambda_s]^\emptyset = 1$, and r_s^i and $p_s^i(\cdot)$ are the probability of existence and single-object density of the i -th Bernoulli component. Thus, a PMB density can be compactly described by the PPP intensity $\lambda_s(\cdot)$ and the parameters of its n_s Bernoulli components, i.e., the existence probabilities r_s^i and the associated single-object densities $p_s^i(\cdot)$.

The GCI fusion rule yields a density [13]

$$f(X) = \frac{(f_1(X))^\omega (f_2(X))^{1-\omega}}{\int (f_1(X))^\omega (f_2(X))^{1-\omega} \delta X} \quad (4)$$

where the denominator is the set integral of the numerator and ensures that $f(\cdot)$ integrates to one. The computation of the GCI rule for PMB densities is intractable. The aim of this paper is to provide an approximation to this fusion rule.

III. APPROXIMATE GCI FUSION OF TWO PMBS

This section presents the proposed approximation to the GCI fusion rule of two PMBs, see (4). Section III-A presents the unnormalised PMB approximation of the power of a PMB. Section III-B presents the main results of this paper showing that the normalised product of two PMB densities results in a PMBM density, which is then the result of the proposed approximation to GCI fusion rule. Section III-C reviews several approaches to project a PMBM density to a PMB density, which is required for subsequent fusion steps. Section III-D proves that the proposed fusion rule minimises a lower bound on the GCI weighted sum of KLDs. Finally, we discuss important aspects of the fusion rule in Section III-E.

A. PMB approximation of the power of a PMB

The computation of the power of a PMB is intractable. Nevertheless, there is the following upper bound to the power of a PMB [34, Eq. (2.12.2)] that holds for $\omega \in [0, 1]$

$$\begin{aligned} (f_1(X))^\omega &= \left(\sum_{X^0 \uplus \dots \uplus X^{n_1} = X} f_1^p(X^0) \prod_{i=1}^{n_1} f_1^i(X^i) \right)^\omega \quad (5) \\ &\leq \sum_{X^0 \uplus \dots \uplus X^{n_1} = X} (f_1^p(X^0))^\omega \prod_{i=1}^{n_1} (f_1^i(X^i))^\omega. \quad (6) \end{aligned}$$

That is, the power of a PMB density is upper bounded by an unnormalised PMB density, which can then be used as an approximation to the PMB. This type of approximation is standard in GCI fusion, for instance, it was used for Gaussian mixtures in [26, Eq. (41)] and for multi-Bernoulli densities in [30, Prop. 2]. In particular, the approximation is accurate if the regions of the single-object space where the main mass of the densities $f_1^p(\cdot)$, $f_1^1(\cdot)$, ..., $f_1^{n_1}(\cdot)$ lie are non-overlapping [30]. In turn, this is more likely to happen in situations with separated objects, high probability of detection and low measurement noise. The resulting form of the power of a PMB is provided in the following lemma.

Lemma 1. *Let $\omega \in [0, 1]$, the ω -power of a PMB density $f_1(\cdot)$ of the form (1) is approximated by the upper bound (6) resulting in*

$$(f_1(X))^\omega \approx \sum_{X^0 \uplus \dots \uplus X^{n_1} = X} (f_1^p(X^0))^\omega \prod_{i=1}^{n_1} (f_1^i(X^i))^\omega \quad (7)$$

$$= \alpha_1 q_1(X) \quad (8)$$

where α is a proportionality constant

$$\alpha_1 = \frac{e^{-\omega \int \lambda_1(x) dx}}{e^{-\int \lambda_1^\omega(x) dx}} \times \prod_{i=1}^{n_1} \left[(1 - r_1^i)^\omega + (r_1^i)^\omega \int (p_1^i(x))^\omega dx \right] \quad (9)$$

and $q_1(\cdot)$ is a PMB density

$$q_1(X) = \sum_{X^0 \uplus \dots \uplus X^{n_1} = X} q_1^p(X^0) \prod_{i=1}^{n_1} q_1^i(X^i) \quad (10)$$

where the PPP density $q_1^p(\cdot)$ has intensity

$$\lambda_{q,1}(x) = (\lambda_1(x))^\omega \quad (11)$$

and the i -th Bernoulli density $q_1^i(\cdot)$ has probability of existence and single-object density given by

$$r_{q,1}^i = \frac{(r_1^i)^\omega \int (p_1^i(x))^\omega dx}{(1 - r_1^i)^\omega + (r_1^i)^\omega \int (p_1^i(x))^\omega dx} \quad (12)$$

$$p_{q,1}^i(x) = \frac{(p_1^i(x))^\omega}{\int (p_1^i(x))^\omega dx}. \quad (13)$$

The proof of Lemma 1 is provided in Appendix A. Performing an analogous approximation with $(f_2(X))^{1-\omega}$, the fused density (4) is given by the normalised product of two PMBs.

B. Normalised product of two PMB densities

Plugging the approximation in Lemma 1 for $(f_1(\cdot))^\omega$ and $(f_2(\cdot))^{1-\omega}$, which yield the PMBs $q_1(\cdot)$ and $q_2(\cdot)$, into (4), the fused density becomes the normalised product of two PMBs

$$q(X) = \frac{q_1(X) q_2(X)}{\int q_1(X) q_2(X) \delta X}$$

$$\propto \sum_{X^0 \uplus \dots \uplus X^{n_1} = X} q_1^p(X^0) \prod_{i=1}^{n_1} q_1^i(X^i)$$

$$\times \sum_{Y^0 \uplus \dots \uplus Y^{n_2} = X} q_2^p(Y^0) \prod_{i=1}^{n_2} q_2^i(Y^i). \quad (14)$$

In this section, we provide a closed-form expression for this product. As we will see, the normalised product of two PMB densities results in a PMBM, where the mixture considers all possible Bernoulli-to-Bernoulli association hypotheses, with the possibility of leaving Bernoulli components unassigned. The Bernoulli components that remain unassigned are associated with the PPP of the other density.

1) *Fused PMBM via assignment sets:* Before providing the expression of the resulting PMBM, we first explain the notation. Given two real-valued functions $f(\cdot)$ and $g(\cdot)$, we use the inner product notation

$$\langle f, g \rangle = \int f(x) g(x) dx. \quad (15)$$

We represent the Bernoulli-to-Bernoulli associations using an assignment set γ between $\{1, \dots, n_1\}$ and $\{1, \dots, n_2\}$. That is, $\gamma \subseteq \{1, \dots, n_1\} \times \{1, \dots, n_2\}$ is such that if $(i, j), (i', j') \in \gamma$ then $j = j'$, and if $(i, j), (i', j) \in \gamma$ then $i = i'$ [35]. These properties ensure that every i and j gets at most one assignment. The set of all possible γ is Γ . It should be noted that the number of possible assignments is

$$|\Gamma| = \sum_{p=0}^{\min(n_1, n_2)} p! \binom{n_1}{p} \binom{n_2}{p} \quad (16)$$

where p goes through the number of assigned objects.

In addition, for a given γ , let $\gamma_1^{u,s}, \dots, \gamma_{n_s-|\gamma|}^{u,s}$ denote the indices of the unassigned Bernoulli components in density $s \in \{1, 2\}$. We also write the assignment set as $\gamma = \{\gamma_1, \dots, \gamma_{|\gamma|}\}$, $\gamma_i = (\gamma_i(1), \gamma_i(2))$. The normalised product of two PMB densities is then given in the following Theorem.

Theorem 2. *The normalised product of the PMB densities $q_1(\cdot)$ and $q_2(\cdot)$ in (14) is a PMBM of the form*

$$q(X) = \sum_{U \uplus W = X} q^p(U) q^{\text{mbm}}(W) \quad (17)$$

where the PPP density is

$$q^p(U) = e^{-\int \lambda_{q,1}(x) \lambda_{q,2}(x) dx} [\lambda_{q,1} \cdot \lambda_{q,2}]^U. \quad (18)$$

The MBM density is

$$q^{\text{mbm}}(W) = \sum_{\gamma \in \Gamma} \rho_\gamma \sum_{X^1 \uplus \dots \uplus X^{n_1} \uplus Y^{\gamma_1^{u,2}} \uplus \dots \uplus Y^{\gamma_{n_2-|\gamma|}^{u,2}} = W}$$

$$\times \prod_{i=1}^{|\gamma|} q_{\gamma_i(1), \gamma_i(2)} \left(X^{\gamma_i(1)} \right)$$

$$\times \prod_{i=1}^{n_1-|\gamma|} q_{\gamma_i^{u,1}, 0} \left(X^{\gamma_i^{u,1}} \right) \prod_{i=1}^{n_2-|\gamma|} q_{0, \gamma_i^{u,2}} \left(Y^{\gamma_i^{u,2}} \right) \quad (19)$$

where the weight ρ_γ of assignment γ is the product of the weights of each Bernoulli component

$$\rho_\gamma \propto \left[\prod_{i=1}^{|\gamma|} \rho_{\gamma_i(1), \gamma_i(2)} \right] \left[\prod_{i=1}^{n_1-|\gamma|} \rho_{\gamma_i^{u,1}, 0} \right] \left[\prod_{i=1}^{n_2-|\gamma|} \rho_{0, \gamma_i^{u,2}} \right] \quad (20)$$

and $q_{i,j}(\cdot)$ is a Bernoulli density with probability of existence $r_{i,j}$, single-object density $p_{i,j}(\cdot)$ and weight $\rho_{i,j}$, which are calculated as follows. For assigned Bernoulli densities, $i \in \{1, \dots, n_1\}$ and $j \in \{1, \dots, n_2\}$, we have that

$$r_{i,j} = \frac{r_{q,1}^i r_{q,2}^j \langle p_{q,1}^i, p_{q,2}^j \rangle}{\rho_{i,j}} \quad (21)$$

$$p_{i,j}(x) = \frac{p_{q,1}^i(x) p_{q,2}^j(x)}{\langle p_{q,1}^i, p_{q,2}^j \rangle} \quad (22)$$

$$\rho_{i,j} = (1 - r_{q,1}^i) (1 - r_{q,2}^j) + r_{q,1}^i r_{q,2}^j \langle p_{q,1}^i, p_{q,2}^j \rangle. \quad (23)$$

For unassigned Bernoulli densities in the first PMB density, with $i \in \{1, \dots, n_1\}$, we have

$$r_{i,0} = \frac{r_{q,1}^i \langle p_{q,1}^i, \lambda_{q,2} \rangle}{\rho_{i,0}} \quad (24)$$

$$p_{i,0}(x) = \frac{p_{q,1}^i(x) \lambda_{q,2}(x)}{\langle p_{q,1}^i, \lambda_{q,2} \rangle} \quad (25)$$

$$\rho_{i,0} = 1 - r_{q,1}^i + r_{q,1}^i \langle p_{q,1}^i, \lambda_{q,2} \rangle. \quad (26)$$

For unassigned Bernoulli densities in the second PMB density, with $j \in \{1, \dots, n_2\}$, we have

$$r_{0,j} = \frac{r_{q,2}^j \langle p_{q,2}^j, \lambda_{q,1} \rangle}{\rho_{0,j}} \quad (27)$$

$$p_{0,j}(x) = \frac{p_{q,2}^j(x) \lambda_{q,1}(x)}{\langle p_{q,2}^j, \lambda_{q,1} \rangle} \quad (28)$$

$$\rho_{0,j} = 1 - r_{q,2}^j + r_{q,2}^j \langle p_{q,2}^j, \lambda_{q,1} \rangle. \quad (29)$$

We prove Theorem 2 in Appendix B.

Example 3. Let us consider the PMBs $q_1(\cdot)$ and $q_2(\cdot)$ shown in Figure 2 (top). The single-object states contain 2-D positions. Both PMBs have three Bernoulli components, with Gaussian single-object densities represented by confidence ellipses. The PPP intensity in both cases is Gaussian with weight 1, mean $[10, 10]^T$ and covariance matrix $20I_2$, covering the whole area of interest. Using (16), the number of possible assignments is $|\Gamma| = 34$. The global hypothesis (assignment set γ) with highest weight is $\gamma = \{(1, 1), (2, 2)\}$. In this hypothesis, the third Bernoulli component in each PMB is left unassigned (associated to the PPP), resulting in $\gamma_1^{u,1} = 3$ and $\gamma_1^{u,2} = 3$. The fused PMB of this global hypothesis has four Bernoulli components and is shown in Figure 2 (bottom). The assigned Bernoulli components give rise to fused Bernoulli components merging the information from the original Bernoulli components. The unassigned Bernoulli components are fused with the PPP adjusting their probabilities of existence, means and covariance matrices.

2) *Fused PMBM in track-oriented form:* Theorem 2 can also be expressed in a track-oriented form using standard PMBM filtering notation [9]. This helps the implementation of the filter as it is possible to leverage available PMBM filter implementations that make use of the track-oriented form. To

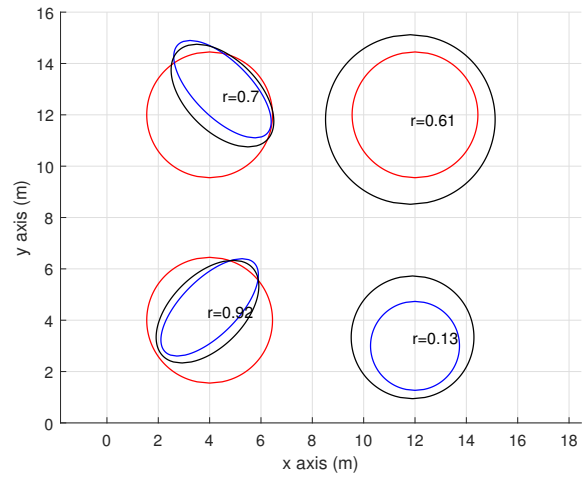
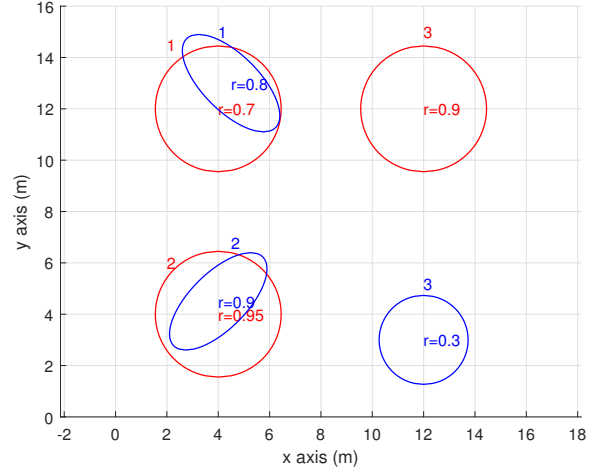


Figure 2: Example fusion of two PMBs $q_1(\cdot)$ (red) and $q_2(\cdot)$ (blue). Both PMBs have three Bernoulli components, indexed by 1, 2 and 3 (top figure). The probability of existence is shown at the center of the 3- σ ellipse representing the mean and covariance matrix. The bottom figure shows the PMB (black) in the most likely hypothesis of the fused PMBM.

do this, we think of $q_1(\cdot)$ as the prior PMB and the Bernoulli components of $q_2(\cdot)$ as the received set of measurements. The fused PMBM then has $n_1 + n_2$ Bernoulli components, obtained by appending the Bernoulli components of $q_2(\cdot)$ to those of $q_1(\cdot)$. In this notation, the assignment set γ is represented with a global hypothesis $a = (a^1, \dots, a^{n_1+n_2})$, where $a^i \in \{1, \dots, h^i\}$ is the index to the local hypothesis for the i -th Bernoulli and h^i is the number of local hypotheses. A local hypothesis assigns the i -th Bernoulli to another Bernoulli in $q_2(\cdot)$ or leaves it unassigned. With this notation, the MBM component of the PMBM can be written as

$$q^{\text{mbm}}(W) \propto \sum_{a \in \mathcal{A}_k} \sum_{X^1 \uplus \dots \uplus X^{n_1+n_2} = W} \prod_{i=1}^{n_1+n_2} \rho^{i,a^i} q^{i,a^i}(X^i) \quad (30)$$

where \mathcal{A}_k is the set of all global hypotheses, and ρ^{i,a^i} and $q^{i,a^i}(\cdot)$ are the weight and Bernoulli density corresponding to local hypothesis a^i in the i -th Bernoulli. The density $q^{i,a^i}(\cdot)$

is characterised by its probability of existence r^{i,a^i} and its single-object density $p^{i,a^i}(\cdot)$.

For each local hypothesis (i, a^i) , there is a set $\mathcal{M}(i, a^i)$ such that $\mathcal{M}(i, a^i) = \{j\}$ if it has been assigned to the j -th Bernoulli in density $q_2(\cdot)$, and $\mathcal{M}(i, a^i) = \emptyset$ if it has been unassigned. Then, the set of all global hypotheses is [36]

$$\mathcal{A}_k = \left\{ (a_1, \dots, a_{n_1+n_2}) : a_i \in \mathbb{N}_{h_i}, \bigcup_{i=1}^{n_1+n_2} \mathcal{M}(i, a_i) = \mathbb{N}_{n_2}, \right. \\ \left. \mathcal{M}(i, a_i) \cap \mathcal{M}(j, a_j) = \emptyset \forall i \neq j \right\} \quad (31)$$

where $\mathbb{N}_n = \{1, \dots, n\}$. The set \mathcal{A}_k ensures the same constraints as the assignment sets $\gamma \in \Gamma$. The following lemma provides the track-oriented form of Theorem 2, providing expressions for $q^{i,a^i}(\cdot)$, ρ^{i,a^i} and $\mathcal{M}(i, a^i)$.

Lemma 4. *The normalised product of the PMB densities $q_1(\cdot)$ and $q_2(\cdot)$ in (14) is a PMBM of the form (17) where the PPP has intensity (18). The MBM density in (19) can also be written in track-oriented form, see (30), as follows. For each Bernoulli component in PMB $q_1(\cdot)$, $i \in \{1, \dots, n_1\}$, there are $h^i = n_2 + 1$ local hypotheses, corresponding to an unassignment hypothesis and an assignment with one of the Bernoulli components in PMB $q_2(\cdot)$. The unassignment hypothesis for the i -th Bernoulli component is characterised by*

$$\mathcal{M}(i, 1) = \emptyset \quad (32)$$

$$r^{i,1} = \frac{r_{q,1}^i \langle p_{q,1}^i, \lambda_{q,2} \rangle}{\rho^{i,1}} \quad (33)$$

$$p^{i,1}(x) = \frac{p_{q,1}^i(x) \lambda_{q,2}(x)}{\langle p_{q,1}^i, \lambda_{q,2} \rangle} \quad (34)$$

$$\rho^{i,1} = 1 - r_{q,1}^i + r_{q,1}^i \langle p_{q,1}^i, \lambda_{q,2} \rangle. \quad (35)$$

The hypothesis assigning Bernoulli component $i \in \{1, \dots, n_1\}$ in $q_1(\cdot)$ to Bernoulli component $i \in \{1, \dots, n_2\}$ in $q_2(\cdot)$ is characterised by

$$\mathcal{M}(i, 1+j) = \{j\} \quad (36)$$

$$r^{i,1+j} = \frac{r_{q,1}^i r_{q,2}^j \langle p_{q,1}^i, p_{q,2}^j \rangle}{\rho^{i,1+j}} \quad (37)$$

$$p^{i,1+j}(x) = \frac{p_{q,1}^i(x) p_{q,2}^j(x)}{\langle p_{q,1}^i, p_{q,2}^j \rangle} \quad (38)$$

$$\rho^{i,1+j} = (1 - r_{q,1}^i) \left(1 - r_{q,2}^j \right) \\ + r_{q,1}^i r_{q,2}^j \int p_{q,1}^i(x) p_{q,2}^j(x) dx. \quad (39)$$

Finally, for Bernoulli components created by the Bernoulli components in $q_2(\cdot)$, with indices $i \in \{n_1 + 1, \dots, n_2\}$, there are two local hypotheses. The first local hypothesis is a non-existent Bernoulli, parameterised by $\mathcal{M}(i, 1) = \emptyset$, $\rho^{i,1} = 1$, $r^{i,1} = 0$. The second local hypothesis represents that the j -th Bernoulli in $q_2(\cdot)$ is unassigned and is parameterised by

$$\mathcal{M}(i, 2) = \{j\} \quad (40)$$

$$r^{i,2} = \frac{r_{q,2}^j \langle p_{q,2}^j, \lambda_{q,1} \rangle}{\rho^{i,2}} \quad (41)$$

$$p^{i,2}(x) = \frac{p_{q,2}^j(x) \lambda_{q,1}(x)}{\langle p_{q,2}^j, \lambda_{q,1} \rangle} \quad (42)$$

$$\rho^{i,2} = 1 - r_{q,2}^j + r_{q,2}^j \langle p_{q,2}^j, \lambda_{q,1} \rangle. \quad (43)$$

The pseudocode summarising the GCI-PMB fusion rule is provided in Algorithm 1.

Algorithm 1 GCI-PMB fusion of two PMB densities.

Input: PMB densities $f_1(\cdot)$ and $f_2(\cdot)$, see (1), fusion parameter $\omega \in [0, 1]$.

Output: Fused PMBM $q(\cdot)$, see (17).

- Approximate ω -power of $f_1(\cdot)$ via Lemma 1, obtaining PMB $q_1(\cdot)$.
 - Approximate $(1 - \omega)$ -power of $f_2(\cdot)$ via Lemma 1, obtaining PMB $q_2(\cdot)$.
 - Calculate the normalised product of $q_1(\cdot)$ and $q_2(\cdot)$ using Lemma 4, obtaining the fused PMBM $q(\cdot)$.
-

C. PMB projection

Once this update is performed, each agent uses the fused PMBM density to continue with the filtering recursion in PMBM form [9], [10]. When another fusion step is required, this PMBM density is projected to a PMB density. Several projection methods can be used:

- Global nearest neighbour (GNN) PMB projection, which selects the most likely assignment [37].
- Track-oriented PMB projection (based on Kullback-Leibler divergence minimisation with auxiliary variables) [9], [36], implemented by selecting the k -best assignments using Murty's algorithm [38] or by belief propagation [39].
- Variational PMB projection [11], [40].

It is also possible to perform the PMB projection immediately after fusion, following one of the methods above.

D. Minimisation of the weighted sum of KLDs

The following lemma indicates that the GCI-PMB fusion rule minimises a lower bound on the GCI weighted sum of KLDs.

Lemma 5. *Given the PMB densities $f_1(\cdot)$ and $f_2(\cdot)$ in (1), the approximate GCI PMB fusion rule arising from Lemma 1 and Theorem 2 provides the density $q(\cdot)$ that minimises the lower bound*

$$L[q] = D \left(q \parallel \frac{q_1 q_2}{\langle q_1, q_2 \rangle} \right) - \log(\alpha_1 \alpha_2 \langle q_1, q_2 \rangle) \quad (44)$$

to the GCI weighted sum of KLDs

$$C[q] = \omega D(q \parallel f_1) + (1 - \omega) D(q \parallel f_2) \quad (45)$$

where α_1 and $q_1(\cdot)$ are given by (9) and (10), and α_2 and $q_2(\cdot)$ are given by same equations but using $f_2(\cdot)$ and $1 - \omega$ instead of $f_1(\cdot)$ and ω .

That is, the GCI fusion rule (4) minimises $C[q]$ whereas the proposed approximate GCI fusion rule minimises its lower bound $L[q] \leq C[q]$.

E. Discussion

This section provides a discussion of the proposed fusion rule, covering its benefits, its comparison with [32], and the extension to PMBM densities. The first benefit is that the fusion rule only requires the approximation in Lemma 1, while all the subsequent steps admit closed-form expressions. Since the PMBM form is kept in the filtering recursion for a large number of multi-object measurement models, including point and extended objects [9], [10], [41], [42], the second benefit is that the fused output can be directly used by each agent to continue with the local filtering recursion. The third benefit is the interpretability of the fused result. The fused PMBM density contains all possible assignments between the Bernoulli components (potential objects) in both PMBs, with the possibility of leaving them unassigned. The unassigned Bernoulli components are fused with the PPP, which represents objects that remain undetected, in the other filter and initiate a new track in the fused PMBM density. This is a natural way of fusing MOF information that intrinsically starts new tracks and performs the association between potential objects. This is in contrast with other existing approaches that use external methods to perform the assignment and initiate new tracks, see for instance [20], [24]. While the PPP component of the PMB is a natural way to account for the presence of undetected objects outside the FoV, the direct application of the proposed GCI fusion rule to sensors with limited FoVs does not yield satisfactory results, as it can lead to an increase of uncertainty [28]. How to apply the proposed fusion rule in this case is explained in Section V.

The proposed fusion rule minimises a lower bound on the GCI-KLD (45) and returns a PMBM. In contrast, the GCI rule in [32] minimises an upper bound and returns a PMB. To do this, the fusion in [32] first divides the PPP of each agent into a number of independent PPPs such that the total number of PPPs plus Bernoulli components is the same for each agent. Then, the algorithm finds the PMB that minimises an upper bound on the weighted KLD across the agents. This KLD upper bound can freely choose the permutations that assign PPP or Bernoulli components across different agents. The proposed way in [32] to obtain these permutations is by fusing the information of 2 agents at a time by minimising a symmetric KLD between the single-object densities, which can be done solving a 2D assignment problem. On the contrary, the proposed method only requires the approximation in Lemma 1 and directly provides the weights of the PMBM global hypotheses. The most likely hypothesis (representing a PMB) can also be computed solving a 2D assignment problem.

The proposed GCI fusion method can in principle be applied to PMBM densities by making the approximation (7) to the PMBM, and then calculating the normalised product of two PMBM densities, which would return a PMBM density (for instance, one can apply the PMB fusion result for each pair of PMBs in the PMBM). There are a number of challenges

though. The first one is that the resulting PMBM would not be in a track-oriented form, which is required for a computationally efficient implementation. It may be possible to design methods to write the fused PMBM in track-oriented form, or perform some type of approximation to achieve this. An additional challenge is that the computational complexity of PMBM GCI fusion can be considerably higher than for PMB fusion due to the possibly high number of global hypotheses. These are topics of future research.

Finally, if there are more than two agents, the multi-agent GCI fusion rule can be applied sequentially by adjusting the fusion weights [33, Table I]. In our case, we must apply a PMB projection, see Section III-C, before each fusion step.

IV. GAUSSIAN GCI-PMB IMPLEMENTATION

In this section, we provide the Gaussian implementation of the fusion rule. In the Gaussian implementation, we assume that the PPP intensity of the s -th node is an unnormalised Gaussian mixture

$$\lambda_s(x) = \sum_{j=1}^{n_s^p} w_s^{p,j} \mathcal{N}(x; \bar{x}_s^{p,j}, P_s^{p,j}), \quad (46)$$

where n_s^p is the number of components, $w_s^{p,j} > 0$, $\bar{x}_s^{p,j}$ and $P_s^{p,j}$ are the weight, mean and covariance matrix of the j -th component, respectively.

The single-object density of the $i \in \{1, \dots, n_s\}$ Bernoulli of the s -th node is Gaussian

$$p_s^i(x) = \mathcal{N}(x; \bar{x}_s^i, P_s^i) \quad (47)$$

where \bar{x}_s^i and P_s^i are the mean and covariance matrix, respectively. Intensities and densities of the forms (46) and (47) naturally arise in PMBM/PMB filtering with linear Gaussian dynamic and measurement models under constant probabilities of survival and detection [9], [10].

Section IV-A explains the PMB approximation of the power of a PMB, Section IV-B explains the GCI rule, and Section IV-C discusses some practical aspects.

A. PMB approximation of the power of a PMB

1) *Power of PPP intensity*: Substituting (46) into (11), the PPP intensity for node 1 is

$$\begin{aligned} \lambda_{q,1}(x) &= \left(\sum_{j=1}^{n_1^p} w_1^{p,j} \mathcal{N}(x; \bar{x}_1^{p,j}, P_1^{p,j}) \right)^\omega \\ &\approx \sum_{j=1}^{n_1^p} \left(w_1^{p,j} \right)^\omega \left(\mathcal{N}(x; \bar{x}_1^{p,j}, P_1^{p,j}) \right)^\omega \\ &= \sum_{j=1}^{n_1^p} \left(w_1^{p,j} \right)^\omega \kappa(\omega, P_1^{p,j}) \mathcal{N}\left(x; \bar{x}_1^{p,j}, \frac{P_1^{p,j}}{\omega}\right) \end{aligned} \quad (48)$$

where

$$\kappa(\omega, P) = \frac{|2\pi P \omega^{-1}|^{1/2}}{|2\pi P| \omega^{1/2}} \quad (49)$$

and we have applied the standard approximation for the exponential of a mixture in [26, Eq. (41)]. Similarly, for the intensity of node 2, we have that

$$\lambda_{q,2}(x) \approx \sum_{j=1}^{n_2^p} \left(w_2^{p,j}\right)^{1-\omega} \kappa\left(1-\omega, P_2^{p,j}\right) \times \mathcal{N}\left(x; \bar{x}_2^{p,j}, \frac{P_2^{p,j}}{1-\omega}\right). \quad (50)$$

2) *Power of Bernoulli density*: Substituting (47) into (12) and (13) yields

$$r_{q,1}^i = \frac{\left(r_1^i\right)^\omega \kappa\left(\omega, P_1^i\right)}{\left(1-r_1^i\right)^\omega + \left(r_1^i\right)^\omega \kappa\left(\omega, P_1^i\right)} \quad (51)$$

$$p_{q,1}^i(x) = \mathcal{N}\left(x; \bar{x}_s^i, \frac{P_s^i}{\omega}\right) \quad (52)$$

where we have used the fact that [26, Eq. (36)]

$$\int \left(p_1^i(x)\right)^\omega dx = \kappa\left(\omega, P_1^i\right). \quad (53)$$

B. GCI rule

The GCI fusion rule for two Gaussian PMB densities is obtained as indicated in the next lemma.

Lemma 6. *Let us consider two PMB densities, denoted by $q_s(\cdot)$ with index $s \in \{1, 2\}$, with Gaussian mixture PPP intensity*

$$\lambda_{q,s}(x) = \sum_{j=1}^{n_{q,s}^p} w_{q,s}^{p,j} \mathcal{N}\left(x; \bar{x}_{q,s}^{p,j}, P_{q,s}^{p,j}\right) \quad (54)$$

and MB characterised by probabilities of existence $r_{q,s}^i$ and single-object densities

$$p_{q,s}^i(x) = \mathcal{N}\left(x; \bar{x}_{q,s}^i, P_{q,s}^i\right) \quad (55)$$

for $i \in \{1, \dots, n_s\}$. The normalised product (14) of these PMB densities is the PMBM in Theorem 2 with density (17). The fused PPP intensity is then given by

$$\lambda_{q,1}(x) \cdot \lambda_{q,2}(x) = \sum_{j_1=1}^{n_{q,1}^p} \sum_{j_2=1}^{n_{q,2}^p} w_{q,1}^{p,j_1} w_{q,2}^{p,j_2} \alpha_{0,0}^{j_1,j_2} \mathcal{N}\left(x; \bar{x}_{0,0}^{j_1,j_2}, P_{0,0}^{j_1,j_2}\right) \quad (56)$$

where

$$\alpha_{0,0}^{j_1,j_2} = \mathcal{N}\left(\bar{x}_{q,1}^{p,j_1}; \bar{x}_{q,2}^{p,j_2}, P_{q,1}^{p,j_1} + P_{q,2}^{p,j_2}\right) \quad (57)$$

$$P_{0,0}^{j_1,j_2} = \left(\left(P_{q,1}^{p,j_1}\right)^{-1} + \left(P_{q,2}^{p,j_2}\right)^{-1}\right)^{-1} \quad (58)$$

$$\bar{x}_{0,0}^{j_1,j_2} = P_{0,0}^{j_1,j_2} \left(\left(P_{q,1}^{p,j_1}\right)^{-1} \bar{x}_{q,1}^{p,j_1} + \left(P_{q,2}^{p,j_2}\right)^{-1} \bar{x}_{q,2}^{p,j_2}\right). \quad (59)$$

For the assigned Bernoulli components, with $i \in \{1, \dots, n_1\}$ and $j \in \{1, \dots, n_2\}$, the resulting Bernoulli density is parameterised by

$$r_{i,j} = \frac{r_{q,1}^i r_{q,2}^j \alpha^{i,j}}{\rho_{i,j}} \quad (60)$$

$$p_{i,j}(x) = \mathcal{N}\left(x; \bar{x}^{i,j}, P^{i,j}\right) \quad (61)$$

$$\rho_{i,j} = \left(1-r_{q,1}^i\right) \left(1-r_{q,2}^j\right) + r_{q,1}^i r_{q,2}^j \alpha^{i,j} \quad (62)$$

where

$$\alpha^{i,j} = \mathcal{N}\left(\bar{x}_{q,1}^i; \bar{x}_{q,2}^j, P_{q,1}^i + P_{q,2}^j\right) \quad (63)$$

$$P^{i,j} = \left(\left(P_{q,1}^i\right)^{-1} + \left(P_{q,2}^j\right)^{-1}\right)^{-1} \quad (64)$$

$$\bar{x}^{i,j} = P^{i,j} \left(\left(P_{q,1}^i\right)^{-1} \bar{x}_{q,1}^i + \left(P_{q,2}^j\right)^{-1} \bar{x}_{q,2}^j\right). \quad (65)$$

For unassigned Bernoulli densities in the first PMB density, with $i \in \{1, \dots, n_1\}$, we have

$$r_{i,0} = \frac{r_{q,1}^i \sum_{j=1}^{n_{q,2}^p} w_{q,2}^{p,j} \alpha_{i,0}^j}{\rho_{i,0}} \quad (66)$$

$$p_{i,0}(x) \propto \sum_{j=1}^{n_{q,2}^p} w_{q,2}^{p,j} \alpha_{i,0}^j \mathcal{N}\left(x; \bar{x}_{i,0}^j, P_{i,0}^j\right) \quad (67)$$

$$\rho_{i,0} = 1 - r_{q,1}^i + r_{q,1}^i \sum_{j=1}^{n_{q,2}^p} w_{q,2}^{p,j} \alpha_{i,0}^{i,j} \quad (68)$$

where

$$\alpha_{i,0}^j = \mathcal{N}\left(\bar{x}_{q,1}^i; \bar{x}_{q,2}^{p,j}, P_{q,1}^i + P_{q,2}^{p,j}\right) \quad (69)$$

$$P_{i,0}^j = \left(\left(P_{q,1}^i\right)^{-1} + \left(P_{q,2}^{p,j}\right)^{-1}\right)^{-1} \quad (70)$$

$$\bar{x}_{i,0}^j = P_{i,0}^j \left(\left(P_{q,1}^i\right)^{-1} \bar{x}_{q,1}^i + \left(P_{q,2}^{p,j}\right)^{-1} \bar{x}_{q,2}^{p,j}\right). \quad (71)$$

For unassigned Bernoulli densities in the second PMB density, with $j \in \{1, \dots, n_2\}$, the results are analogous to (66)-(71) with indices changed accordingly to obtain $r_{0,j}$, $p_{0,j}(\cdot)$, $\rho_{0,j}$.

The proof of this lemma is direct by using Theorem 2 and the identity for the product of two Gaussian densities [43, Eq. (11)]. Finally, the PMB projection for the Gaussian implementation also does moment matching to keep each single-object posterior as Gaussian [9], [36].

C. Practical aspects

As the result of GCI-PMB fusion is a PMBM, it is important to limit the number of global hypotheses, Bernoulli components and PPP components for practical implementation. Each agent already performs these operations when running its PMB/PMBM filter but it is also required when performing the fusion rule. This section explains global hypothesis pruning, gating, and pruning-merging of PPP components when performing GCI-PMB fusion.

A GCI-PMB fusion rule implementation requires pruning global hypotheses resulting from Lemma 4. This can be done, for example, via Murty's algorithm or variants [38], [44] or Gibbs sampling [7]. These standard approaches can be used because, as a result of PMB fusion, the weight of each global hypothesis can be factorised as the product of the weights of the local association hypotheses. Gating is a standard mechanism to lower the number of data association hypotheses [45]. In

standard PMBM filtering, the gating between a measurement z and a certain Bernoulli component is performed using the square Mahalanobis distance $(z - \hat{z})^T S^{-1} (z - \hat{z})$ where \hat{z} and S are the predicted measurement and its covariance matrix [45]. This is done because the local hypothesis weight depends on this distance.

In contrast, in GCI-PMB fusion, the weight of the local hypothesis depends on $\alpha^{i,j}$ in (63) which, in turn, depends on the square Mahalanobis distance [26]

$$d^{i,j} = \left(\bar{x}_{q,1}^i - \bar{x}_{q,2}^j \right)^T \left(P_{q,1}^i + P_{q,2}^j \right)^{-1} \left(\bar{x}_{q,1}^i - \bar{x}_{q,2}^j \right). \quad (72)$$

Given a gating threshold Γ_f , if $d^{i,j} < \Gamma_f$, then Bernoulli i can be assigned to Bernoulli j . The same logic is used to assign PPP components to Bernoulli components (in the unassigned local hypotheses).

To lower the number of PPP components, we use pruning and merging after both the local update and the GCI fusion step. Due to the approximation in (48), it is particularly important to merge similar PPP components, as the approximation improves if the Gaussian densities are well separated [26]. In the simulations in Section VI, each agent also prunes global hypotheses and Bernoulli components after the local update and the GCI fusion step. Due to the approximation (7), recycling [46] and merging of Bernoulli components after the GCI fusion step may also help improve performance.

V. APPLICATION TO SENSORS WITH LIMITED FOVS

In this section, we explain one approach to apply the proposed GCI-PMB fusion rule with sensors with limited FoVs. The approach is based on PMB partitioning followed by GCI-PMB fusion in different areas. The partitioning and fusion algorithm is explained in Section V-A. Section V-B explains how to assign Bernoulli components to each partition.

A. Partitioning and fusion

When we consider the GCI fusion of two multi-object densities obtained by sensors with limited FoVs, there can be an increase of uncertainty in those areas which are observed by one sensor but not by the other [28]. This is due to the fact that GCI provides a geometric average between two multi-object densities. Therefore, if one of them has little information about an area, but the other has accurate information about an area, the GCI rule would increase the uncertainty unless we set ω to only consider the information of the sensor with relevant information. This situation gets worse if there are multiple agents with limited FoVs. One solution to this phenomenon proposed in [28] is that each sensor uses an uninformative density outside its FoV. Then, independent fusion is used in the area which is observed by one sensor but not by the other. The GCI rule is only used for the area that is within the FoVs of both sensors.

Based on these insights, we propose the following approach to handle limited FoVs. We first divide the single-object space into three areas $A_0, A_1, A_2 \subseteq \mathbb{R}^{n_x}$, where

- A_1 is the area that contains the FoV of sensor 1 minus the FoV of sensor 2.

- A_2 is the area that contains the FoV of sensor 2 minus the FoV of sensor 1.
- $A_0 = \mathbb{R}^{n_x} \setminus (A_1 \cup A_2)$ is the union of the joint FoV and the area that is outside the FoV of both sensors.

We then assign each Bernoulli component $f_s^i(\cdot)$ to one of these areas, and denote these as $f_s^{i,j}(\cdot)$ for $j \in \{0, 1, 2\}$ and $i = \{1, \dots, n_{s,j}\}$ where $n_{s,j}$ is the number of Bernoulli components in area A_j for sensor s . How to perform this assignment will be explained in Section V-B.

Then, we write each PMB density as the union of three PMB densities

$$f_s(X) = \sum_{W^0 \uplus W^1 \uplus W^2 = X} \prod_{j=0}^2 f_s^{\text{pmb},j}(W^j) \quad (73)$$

where

$$f_s^{\text{pmb},j}(W^i) = \sum_{X^0 \uplus \dots \uplus X^{n_s} = X} f_s^{p,j}(X^0) \prod_{i=1}^{n_{s,j}} f_s^{i,j}(X^i) \quad (74)$$

and the intensity of the PPP $f_s^{p,j}(\cdot)$ is $\lambda_s^j(x) = \lambda_s(x) \chi_{A_j}(x)$, where $\chi_{A_j}(\cdot)$ is the indicator function on A_j . That is, it is the intensity constrained to each of the areas. It is important to note that writing the PMB (1) as (73)-(74) is an exact operation.

The next step is to use the GCI-PMB fusion rule to independently fuse the two PMBs in each area with these settings:

- Fusion of $f_1^{\text{pmb},0}(\cdot)$ with $f_2^{\text{pmb},0}(\cdot)$ with $\omega \in (0, 1)$, typically $\omega = 1/2$, using Theorem 2, yielding a PMBM $q^{\text{pmbm},0}(\cdot)$.
- Fusion of $f_1^{\text{pmb},1}(\cdot)$ with $f_2^{\text{pmb},1}(\cdot)$ with $\omega = 1$, resulting in $f_1^{\text{pmb},1}(\cdot)$.
- Fusion of $f_1^{\text{pmb},2}(\cdot)$ with $f_2^{\text{pmb},2}(\cdot)$ with $\omega = 0$, resulting in $f_2^{\text{pmb},2}(\cdot)$.

That is, we set ω to either 0 or 1 if only one of the sensors clearly has more accurate information than the other in the associated area. The resulting fused density is

$$q(X) = \sum_{W^0 \uplus W^1 \uplus W^2 = X} q^{\text{pmbm},0}(W^0) \times f_1^{\text{pmb},1}(W^1) f_2^{\text{pmb},2}(W^2) \quad (75)$$

It should be noted that this density is a PMBM. It can be written in the PMBM standard form [10] by first noticing that its PPP intensity corresponds to the sum of the intensities of the PPPs of $q^{\text{pmbm},0}(\cdot)$, $f_1^{\text{pmb},1}(\cdot)$ and $f_2^{\text{pmb},2}(\cdot)$, and then appending the Bernoulli components in $f_1^{\text{pmb},1}(\cdot)$ and $f_2^{\text{pmb},2}(\cdot)$ to all the multi-Bernoulli components in the mixture.

B. Bernoulli assignment

In this section, we explain how to assign the Bernoulli components of sensors 1 and 2 to areas A_0, A_1 and A_2 . A simple option would be to assign each Bernoulli to the area that contains most of its probability. However, this can lead to missed object problems at the border of the areas if two Bernoulli components that represent the same object are associated to different areas.

A better alternative is cluster Bernoulli components of both sensors by similarity and assign all the Bernoulli components in each cluster to the same area. To do this, we first compute a distance between the Bernoulli components in one sensor and the other sensor, e.g., using the square Mahalanobis distance in (72). If two Bernoulli components are closer than a threshold, we consider they can be assigned. Then, the clusters are given by pairs of subsets of the Bernoulli components in sensor 1 and in sensor 2 in which there can be assignments. These can be computed by first obtaining the adjacency matrix of the (unweighted) bipartite graph formed by the Bernoulli components, where there is an edge if the Bernoulli components can be assigned. Then, the clusters are the disjoint components in this graph, which can be computed via the reverse Cuthill-McKee algorithm [47].

VI. SIMULATIONS

In this section, we evaluate the performance of the GCI PMB fusion rule for distributed MOF via numerical simulations. We first consider a scenario with two agents. Then we consider a scenario with four agents with limited FoVs. We compare the following distributed PMBM-PMB¹ filter variants, implemented with both GCI and AA fusion.

- Distributed PMBM (DPMBM) filter: each agent runs a PMBM filter with a variational PMB projection with the most likely assignment [40, Sec. V.B] before applying the fusion step.
- DPMB-TO (distributed PMB track oriented) filter: each agent runs a PMB filter performing a track-oriented PMB projection [9], [36] after each update and fusion step.
- DPMB-V: each agent runs a PMB filter performing a variational PMB projection with the most likely assignment [40, Sec. V.B] after each update and after the fusion rule.
- DPMB-GNN: each agent runs a PMB filter with the best global nearest neighbour (GNN) hypothesis for each update and fusion.
- DPMB-KUB: each agent runs a track-oriented PMB filter, and uses the KLD upper bound (KUB) fusion rule in [32, Sec. V.B]. This method is only valid for GCI fusion.
- Centralised PMBM: sequential update with the measurements of each agent.

A. Scenario 1

The scenario has two agents tracking point objects, and the fusion rule is performed every N_f time steps. The parameters of the algorithms are the following. The PMBM/PMB implementation follows the one in [10]. The filters propagate a PPP with maximum 30 components, pruning threshold 10^{-5} and merging threshold 0.1. The threshold for pruning multi-Bernoulli densities is 10^{-4} . For data association, we use gating with threshold 20 and Murty's algorithm with 200 hypotheses. Bernoulli components with a probability of existence lower than 10^{-5} are discarded. PMBM pruning and merging are performed before and after each VPMB projection to lower

¹Matlab code of the proposed algorithms is available at <https://github.com/Agarciafernandez/MTT>.

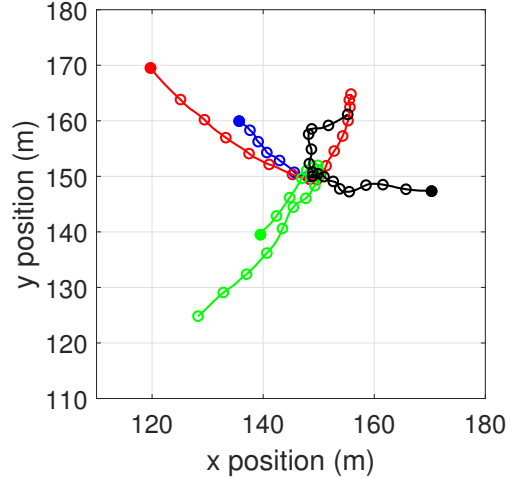


Figure 3: Scenario 1, similar to [10]. There are four objects that get in close proximity in the middle of the simulation. All objects are born at the beginning of the simulation and the blue one dies at time step 40. The object positions every 10 time steps are marked with a circle, and the initial positions with filled circles.

computational cost. The VPMB projection is done with a maximum of 10 iterations, and a convergence threshold 0.1.

The GCI fusion rule has parameter $\omega = 1/2$, gating with threshold $\Gamma_f = 20$ and Murty's algorithm with 200 hypotheses. For comparison purposes, we consider the AA fusion rule for PMB/PMBM filtering [24]. The AA fusion rule has parameter $\omega = 1/2$ and we have implemented a Bernoulli-to-Bernoulli association method based on the Mahalanobis distance (other options are possible [14]). That is, we start with all Bernoulli components being unassigned. Then, we go through all Bernoulli components of agent 1 and compute the Mahalanobis distance with all means of the unassigned Bernoulli components in agent 2. If the minimum square distance is lower than a threshold $\Gamma_{aa} = 5$, these Bernoulli components are assigned, and belong to the same track in a PMBM density structure [9].

The single-object state is $x = [p_x, \dot{p}_x, p_y, \dot{p}_y]^T$ containing its position and velocity. Each object moves with a nearly-constant velocity model with sampling interval $\tau = 1$ and noise covariance parameter 0.01 [10]. The probability of survival is 0.99. The birth model is a PPP with Gaussian intensity with mean $[100, 0, 100, 0]^T$ and covariance matrix $\text{diag}([150^2, 1, 150^2, 1])$. The expected number of new born targets is 3 at time step 1 and 0.005 in the rest of the time steps. There are 81 time steps in the simulations and the ground truth object trajectories are shown in Figure 3.

The agents measure the object positions with additive zero-mean Gaussian noise with covariance matrix $R = 4I$, and a probability of detection $p^D = 0.9$. Clutter is PPP distributed with clutter intensity is $\lambda^C(z) = \bar{\lambda}^C u_A(z)$ where $u_A(z)$ is a uniform density in $A = [0, 300] \times [0, 300]$ and $\bar{\lambda}^C = 10$.

MOF performance is evaluated via Monte Carlo simulation with 100 runs. For each agent, we calculate the error in the estimated set of object positions using generalised optimal sub-pattern assignment (GOSPA) metric with parameters $\alpha = 2$,

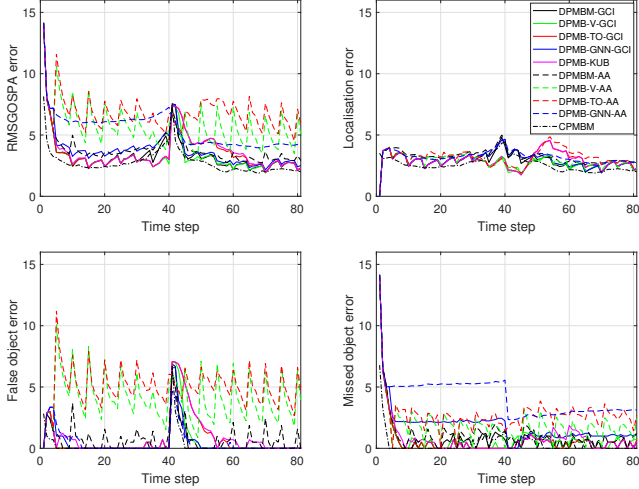


Figure 4: RMS-GOSPA errors at each time step for $N_f = 5$ (Scenario 1). When the agents perform information fusion the error decreases. Among the distributed filters, DPMB-V-GCI and DPMBM-GCI have the best performance.

$p = 2$ and $c = 10$ [35]. We first analyse the case $N_f = 5$, which means the agents fuse their information every 5 time steps. The root mean square GOSPA (RMS-GOSPA) errors at each time step, considering both agents, are shown in Figure 4. This figure also shows the decomposition of the GOSPA metric into localisation cost, missed object cost and false object cost. As expected, the best performance is obtained by the centralised filter, the CPMBM. Among the distributed filters, the DPMB-V-GCI and DPMBM-GCI are the best performing filters. DPMB-TO-GCI performs well before the objects get in close proximity but then the error is higher than the best performing filters due to an increase in false objects. AA filter variants also perform well but they show a higher number of false objects, which increases their GOSPA errors. The GNN versions of the filters perform worse due to a higher number of missed objects. This is expected since the GNN filters only take into account the best global hypothesis, both in the update and in the information fusion step. We can see that every 5 time steps there is a reduction in the error in the distributed filters. This corresponds to the time steps when there is a data fusion step.

We also show the RMS-GOSPA errors across all time steps for $N_f \in \{1, 5, 10\}$ in Table I. As expected, the best performing filter is the CPMBM filter. The best performing distributed filters are DPMBM-GCI and DPMB-V. For these filters (and also DPMB-TO-GCI) lowering N_f increases performance, which is reasonable since there are more fusion steps. DPMB-TO-GCI exhibits higher error due to some track coalescence when targets get in close proximity and then separate. DPMB-GNN-GCI has a higher error due to missed targets. Generally, AA performs worse than GCI in this scenario. We should recall that Bernoulli-to-Bernoulli association (with the possibility of leaving Bernoulli components unassigned) is a natural part of the GCI fusion rule, as shown in Theorem 2. However, AA does not have a Bernoulli-to-Bernoulli association step as a fundamental step of the algorithm, but it must be performed

Table I: RMS-GOSPA errors across all time steps

Fusion rule	GCI			AA			
	N_f	1	5	10	1	5	10
DPMBM		3.34	3.77	3.96	4.15	4.16	4.09
DPMB-V		3.45	3.69	3.87	5.40	5.90	5.22
DPMB-TO		3.77	4.02	4.16	8.95	6.93	6.07
DPMB-GNN		5.20	4.17	4.49	5.63	5.64	5.64
DPMB-KUB		4.88	4.07	4.20	-	-	-
CPMBM		2.99					

via an external procedure to achieve good performance. It is likely that this difference contributes to the better performance of GCI in these simulations. DPMB-KUB works worse than DPMBM, DPMB-V and DPMB-TO with the GCI rule, but it works better than DPMB-GNN and the AA variants (except DPMBM-AA).

B. Scenario 2

This experiment is based on the scenario shown in Figure 5, which contains 4 agents with limited FoVs. The GCI coefficients to perform the fusion rule sequentially are those provided in [33, Table I]. All the algorithms have been implemented with the partitioning approach described in Section V, considering the union of the FoVs of the agents for which we have already performed the fusion, as was done in [28, Alg. 1]. All agents fuse their information every $N_f = 5$ time steps. We have not managed to get DPMB-UBK working properly in this scenario so its results are omitted.

In this scenario, the filters consider a maximum of 100 global hypotheses, and a maximum of 10 PPP components. The GCI-fusion rule also uses 100 global hypotheses with gating threshold 20. Merging of PPP components is performed in their square Mahalanobis distance is smaller than 4. After each PMB projection, we perform recycling with threshold 0.01. We also perform merging of two Bernoulli components if their square Mahalanobis distance is smaller than 4, and the probability that there are two objects after the merging is smaller than 0.01. The probability of existence of the merged Bernoulli components is their sum, which matches the PHD, capped to one.

The single-object state, dynamic model and probability of survival are the same as in the previous section. The birth model is a PPP with intensity

$$\lambda^B(x) = \sum_{q=1}^4 w_k^{b,q} \mathcal{N}(x; \bar{x}^{b,q}, P^{b,q}) \quad (76)$$

where $w_0^{b,q} = 0.75$, $w_k^{b,q} = 0.01$ for $k > 0$, $P^{b,q} = \text{diag}([10^2, 1, 10^2, 1])$, $\bar{x}^{b,1} = [75, 2, 225, -2]^T$, $\bar{x}^{b,2} = [225, -2, 225, -2]^T$, $\bar{x}^{b,3} = [75, 1, 75, 2]^T$, and $\bar{x}^{b,4} = [225, -1, 75, 2]^T$. There is a Gaussian birth component in the FoV of each sensors.

The agents measure the object positions with zero-mean Gaussian noise with covariance $R = 4I$. The probability of detection of sensor s , with field of view $\text{FoV}_s \subset \mathbb{R}^{n_x}$, is

$$p_s^D(x) = \begin{cases} p^D & x \in \text{FoV}_s \\ 0 & \text{otherwise} \end{cases} \quad (77)$$

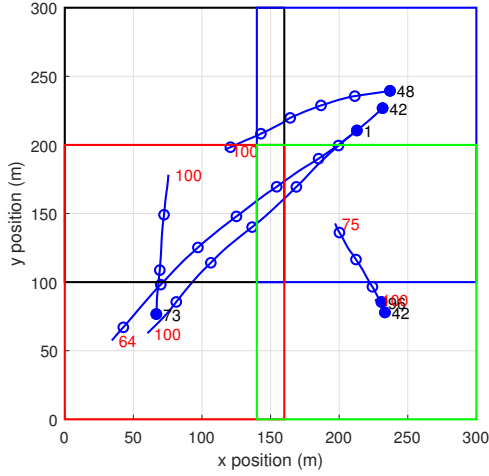


Figure 5: Scenario 2 considering 4 agents with limited FoVs and 100 time steps. The FoV of each agent is a rectangle shown with a different colour. There are six objects, whose positions are marked every 10 time steps with a circle, and the initial positions with filled circles. The initial time step of each object is written in black next to its initial position. The final time step is written in red next to its final position.

with $p^D = 0.9$. Clutter for each sensor is a PPP with uniform intensity in the FoV of each sensor (in the single-measurement space \mathbb{R}^{n_z}) with $\bar{\lambda}^C = 10$. For each single-object Gaussian update, all filters approximate the state-dependent $p_s^D(\cdot)$ as a constant given by its expected value. This is approximately computed by Monte Carlo integration, sampling from the prior, with 100 samples.

At each time step, all agents estimate the set of objects. The root mean square GOSPA (RMS-GOSPA) errors and their decompositions at each time step, considering all agents, using Monte Carlo simulation with 100 runs is shown in Figure 6. The centralised PMBM filter provides the lowest errors. After 5 time steps, the distributed filters improve performance, as the exchange of information happens every 5 time steps. DPMBM-GCI and DPMB-V-GCI have the best performance among the distributed filters. We can see that a main difference between the centralised solution and these distributed filters is in the localisation error, which is higher in the distributed filters. Nevertheless, when agents exchange their information, the localisation error is close to the centralised implementation. False and missed objects tend to linger more in the distributed filters, also due to the delay in the exchange of information. The filter with worse performance is DPMB-GNN-AA, especially due to an increase in the missed object error. Overall, the filters with the GCI rule perform better than those with AA.

VII. CONCLUSIONS

This paper has derived an approximate GCI fusion rule for PMB densities. The only approximation involved is to approximate the power of a PMB by an unnormalised PMB, which is an upper bound. The rest of the GCI fusion rule is in closed form and yields a PMBM that accounts for all possible assignments of Bernoulli components among the two PMB densities. The proposed fusion rule is applicable to any PMB filter, for instance, (track-oriented) PMB filter [9],

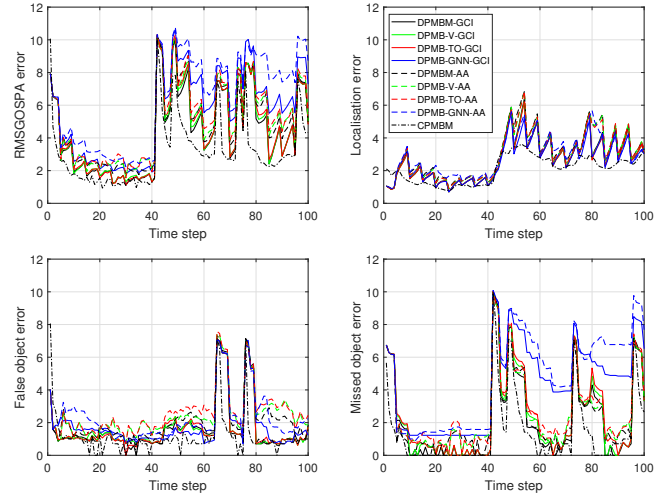


Figure 6: RMS-GOSPA errors at each time step for $N_f = 5$ (Scenario 2). Among the distributed filters, DPMB-V-GCI and DPMBM-GCI have the best performance.

(measurement-oriented) PMB filter [9], variational PMB filter [11], PMB filters for extended object tracking [40] or PMB filters for co-existing point and extended object tracking [48]. The fusion rule can also be applied to any PMBM filter by performing a PMB projection beforehand. The fusion rule has also been extended to deal with sensors with limited FoVs by applying different fusion coefficients in different areas.

Future work includes the application of this fusion rule to large networks via consensus [26] and the extension of this fusion rule to PMBMs. Another line of future work is the distributed recovery of trajectory information by each agent, for instance, using the sequence of filtered PMB densities and backward simulation [22].

REFERENCES

- [1] S. Wei, M. Liang, and F. Meyer, “A new architecture for neural enhanced multiobject tracking,” in *27th International Conference on Information Fusion*, 2024, pp. 1–8.
- [2] D. Cataldo, L. Gentile, S. Ghio, E. Giusti, S. Tomei, and M. Martorella, “Multibistatic radar for space surveillance and tracking,” *IEEE Aerospace and Electronic Systems Magazine*, vol. 35, no. 8, pp. 14–30, 2020.
- [3] A. G. Hem, M. Baerveldt, and E. F. Brekke, “PMBM filtering with fusion of target-provided and exteroceptive measurements: Applications to maritime point and extended object tracking,” *IEEE Access*, vol. 12, pp. 55 404–55 423, 2024.
- [4] S. Su, S. Han, Y. Li, Z. Zhang, C. Feng, C. Ding, and F. Miao, “Collaborative multi-object tracking with conformal uncertainty propagation,” *IEEE Robotics and Automation Letters*, vol. 9, no. 4, pp. 3323–3330, 2024.
- [5] J. Wang, Y. Zeng, S. Wei, Z. Wei, Q. Wu, and Y. Savaria, “Multi-sensor track-to-track association and spatial registration algorithm under incomplete measurements,” *IEEE Transactions on Signal Processing*, vol. 69, pp. 3337–3350, 2021.
- [6] R. P. S. Mahler, *Advances in Statistical Multisource-Multitarget Information Fusion*. Artech House, 2014.
- [7] B. N. Vo, B. T. Vo, and H. G. Hoang, “An efficient implementation of the generalized labeled multi-Bernoulli filter,” *IEEE Transactions on Signal Processing*, vol. 65, no. 8, pp. 1975–1987, April 2017.
- [8] S. Reuter, B.-T. Vo, B.-N. Vo, and K. Dietmayer, “The labeled multi-Bernoulli filter,” *IEEE Transactions on Signal Processing*, vol. 62, no. 12, pp. 3246–3260, June 2014.

- [9] J. L. Williams, "Marginal multi-Bernoulli filters: RFS derivation of MHT, JIPDA and association-based MeMber," *IEEE Transactions on Aerospace and Electronic Systems*, vol. 51, no. 3, pp. 1664–1687, July 2015.
- [10] A. F. García-Fernández, J. L. Williams, K. Granström, and L. Svensson, "Poisson multi-Bernoulli mixture filter: direct derivation and implementation," *IEEE Transactions on Aerospace and Electronic Systems*, vol. 54, no. 4, pp. 1883–1901, Aug. 2018.
- [11] J. L. Williams, "An efficient, variational approximation of the best fitting multi-Bernoulli filter," *IEEE Transactions on Signal Processing*, vol. 63, no. 1, pp. 258–273, Jan. 2015.
- [12] A. F. García-Fernández, Y. Xia, K. Granström, L. Svensson, and J. L. Williams, "Gaussian implementation of the multi-Bernoulli mixture filter," in *Proceedings of the 22nd International Conference on Information Fusion*, 2019, pp. 1–8.
- [13] R. P. S. Mahler, "Optimal/robust distributed data fusion: a unified approach," in *Proceedings of the SPIE*, vol. 4052, 2000, pp. 128–138.
- [14] T. Li, X. Wang, Y. Liang, and Q. Pan, "On arithmetic average fusion and its application for distributed multi-Bernoulli multitarget tracking," *IEEE Transactions on Signal Processing*, vol. 68, pp. 2883–2896, 2020.
- [15] L. Gao, G. Battistelli, and L. Chisci, "Multiobject fusion with minimum information loss," *IEEE Signal Processing Letters*, vol. 27, pp. 201–205, 2020.
- [16] S. Li, G. Battistelli, L. Chisci, W. Yi, B. Wang, and L. Kong, "Computationally efficient multi-agent multi-object tracking with labeled random finite sets," *IEEE Transactions on Signal Processing*, vol. 67, no. 1, pp. 260–275, 2019.
- [17] T. Kropfreiter and F. Hlawatsch, "A probabilistic label association algorithm for distributed labeled multi-Bernoulli filtering," in *IEEE 23rd International Conference on Information Fusion*, 2020, pp. 1–8.
- [18] K. Shen, P. Dong, Z. Jing, and H. Leung, "Consensus-based labeled multi-Bernoulli filter for multitarget tracking in distributed sensor network," *IEEE Transactions on Cybernetics*, vol. 52, no. 12, pp. 12722–12733, 2022.
- [19] L. Gao, G. Battistelli, and L. Chisci, "Fusion of labeled RFS densities with minimum information loss," *IEEE Transactions on Signal Processing*, vol. 68, pp. 5855–5868, 2020.
- [20] S. Li, W. Yi, R. Hoseinnezhad, G. Battistelli, B. Wang, and L. Kong, "Robust distributed fusion with labeled random finite sets," *IEEE Transactions on Signal Processing*, vol. 66, no. 2, pp. 278–293, 2018.
- [21] J. Wei, F. Luo, J. Qi, and X. Luo, "Distributed fusion of labeled multi-Bernoulli filters based on arithmetic average," *IEEE Signal Processing Letters*, vol. 31, pp. 656–660, 2024.
- [22] Y. Xia, L. Svensson, A. F. García-Fernández, J. L. Williams, D. Svensson, and K. Granström, "Multiple object trajectory estimation using backward simulation," *IEEE Transactions on Signal Processing*, vol. 70, pp. 3249–3263, 2022.
- [23] T. Li, J. M. Corchado, and S. Sun, "Partial consensus and conservative fusion of Gaussian mixtures for distributed PHD fusion," *IEEE Transactions on Aerospace and Electronic Systems*, vol. 55, no. 5, pp. 2150–2163, Oct. 2019.
- [24] T. Li, Y. Xin, Z. Liu, and K. Da, "Best fit of mixture for multi-sensor Poisson multi-Bernoulli mixture filtering," *Signal Processing*, vol. 202, pp. 1–14, 2023.
- [25] M. Üney, D. E. Clark, and S. J. Julier, "Distributed fusion of PHD filters via exponential mixture densities," *IEEE Journal of Selected Topics in Signal Processing*, vol. 7, no. 3, pp. 521–531, June 2013.
- [26] G. Battistelli, L. Chisci, C. Fantacci, A. Farina, and A. Graziano, "Consensus CPHD filter for distributed multitarget tracking," *IEEE Journal of Selected Topics in Signal Processing*, vol. 7, no. 3, pp. 508–520, June 2013.
- [27] H. Kim, K. Granström, L. Gao, G. Battistelli, S. Kim, and H. Wymeersch, "5G mmwave cooperative positioning and mapping using multi-model PHD filter and map fusion," *IEEE Transactions on Wireless Communications*, vol. 19, no. 6, pp. 3782–3795, 2020.
- [28] B. Wang, S. Li, G. Battistelli, L. Chisci, and W. Yi, "Multi-agent fusion with different limited fields-of-view," *IEEE Transactions on Signal Processing*, vol. 70, pp. 1560–1575, 2022.
- [29] M. B. Guldogan, "Consensus Bernoulli filter for distributed detection and tracking using multi-static Doppler shifts," *IEEE Signal Processing Letters*, vol. 21, no. 6, pp. 672–676, 2014.
- [30] B. Wang, W. Yi, R. Hoseinnezhad, S. Li, L. Kong, and X. Yang, "Distributed fusion with multi-Bernoulli filter based on generalized covariance intersection," *IEEE Transactions on Signal Processing*, vol. 65, no. 1, pp. 242–255, Jan. 2017.
- [31] C. Lv, J. Zhu, and Z. Peng, "Generalised covariance intersection-gamma Gaussian inverse Wishart-Poisson multi-Bernoulli mixture: An intelligent multiple extended target tracking scheme for mobile aquaculture sensor networks," *IET Wireless Sensor Systems*, vol. 14, no. 1-2, pp. 1–19, 2024.
- [32] M. Fröhle, K. Granström, and H. Wymeersch, "Decentralized Poisson multi-Bernoulli filtering for vehicle tracking," *IEEE Access*, vol. 8, pp. 126414–126427, 2020.
- [33] M. Günay, U. Orguner, and M. Demirekler, "Chernoff fusion of Gaussian mixtures based on sigma-point approximation," *IEEE Transactions on Aerospace and Electronic Systems*, vol. 52, no. 6, pp. 2732–2746, 2016.
- [34] G. H. Hardy, J. E. Littlewood, and G. P. Lya, *Inequalities*. Cambridge University Press, 1934.
- [35] A. S. Rahmathullah, A. F. García-Fernández, and L. Svensson, "Generalized optimal sub-pattern assignment metric," in *20th International Conference on Information Fusion*, 2017, pp. 1–8.
- [36] A. F. García-Fernández, L. Svensson, J. L. Williams, Y. Xia, and K. Granström, "Trajectory Poisson multi-Bernoulli filters," *IEEE Transactions on Signal Processing*, vol. 68, pp. 4933–4945, 2020.
- [37] D. F. Crouse, "On implementing 2D rectangular assignment algorithms," *IEEE Transactions on Aerospace and Electronic Systems*, vol. 52, no. 4, pp. 1679–1696, August 2016.
- [38] K. G. Murty, "An algorithm for ranking all the assignments in order of increasing cost," *Operations Research*, vol. 16, no. 3, pp. 682–687, 1968.
- [39] J. Williams and R. Lau, "Approximate evaluation of marginal association probabilities with belief propagation," *IEEE Transactions on Aerospace and Electronic Systems*, vol. 50, no. 4, pp. 2942–2959, Oct. 2014.
- [40] Y. Xia, K. Granström, L. Svensson, M. Fatemi, A. F. García-Fernández, and J. L. Williams, "Poisson multi-Bernoulli approximations for multiple extended object filtering," *IEEE Transactions on Aerospace and Electronic Systems*, vol. 58, no. 2, pp. 890–906, 2022.
- [41] K. Granström, M. Fatemi, and L. Svensson, "Poisson multi-Bernoulli mixture conjugate prior for multiple extended target filtering," *IEEE Transactions on Aerospace and Electronic Systems*, vol. 56, no. 1, pp. 208–225, Feb. 2020.
- [42] A. F. García-Fernández, Y. Xia, and L. Svensson, "Poisson multi-Bernoulli mixture filter with general target-generated measurements and arbitrary clutter," *IEEE Transactions on Signal Processing*, vol. 71, pp. 1895–1906, 2023.
- [43] J. L. Williams and P. S. Maybeck, "Cost-function-based Gaussian mixture reduction for target tracking," in *Proceedings of the Sixth International Conference of Information Fusion*, July 2003, pp. 1047–1054.
- [44] C. R. Pedersen, L. R. Nielsen, and K. A. Andersen, "An algorithm for ranking assignments using reoptimization," *Computers & Operations Research*, vol. 35, no. 11, pp. 3714–3726, 2008.
- [45] S. Challa, M. R. Morelande, D. Musicki, and R. J. Evans, *Fundamentals of Object Tracking*. Cambridge University Press, 2011.
- [46] J. L. Williams, "Hybrid Poisson and multi-Bernoulli filters," in *15th International Conference on Information Fusion*, 2012, pp. 1103–1110.
- [47] A. George and J. W. Liu, *Computer Solutions of Large Sparse Positive Definite Systems*. Prentice-Hall, 1981.
- [48] A. F. García-Fernández, J. L. Williams, L. Svensson, and Y. Xia, "A Poisson multi-Bernoulli mixture filter for coexisting point and extended targets," *IEEE Transactions on Signal Processing*, vol. 69, pp. 2600–2610, 2021.

Supplemental material: “Distributed Poisson multi-Bernoulli filtering via generalised covariance intersection”

APPENDIX A

In this appendix, we prove Lemma 1. From Approximation (7), the ω -power of the PPP density is

$$\begin{aligned} (f_1^p(X^0))^\omega &= e^{-\omega \int \lambda_1(x) dx} [\lambda_1^\omega]^X \\ &= \frac{e^{-\omega \int \lambda_1(x) dx}}{e^{-\int \lambda_1^\omega(x) dx}} e^{-\int \lambda_1^\omega(x) dx} [\lambda_1^\omega]^X \\ &= \frac{e^{-\omega \int \lambda_1(x) dx}}{e^{-\int \lambda_1^\omega(x) dx}} q_1^p(X). \end{aligned} \quad (78)$$

On the other hand, the ω -power of the i -th Bernoulli density is

$$\begin{aligned} (f_1^i(X^i))^\omega &= \begin{cases} (1 - r_s^i)^\omega & X = \emptyset \\ (r_s^i)^\omega (p_s^i(x))^\omega & X = \{x\} \\ 0 & \text{otherwise.} \end{cases} \\ &= \begin{cases} (1 - r_s^i)^\omega & X = \emptyset \\ (r_s^i)^\omega p_{q,1}^i(x) \int (p_1^i(x))^\omega dx & X = \{x\} \\ 0 & \text{otherwise.} \end{cases} \end{aligned} \quad (79)$$

The above equation can be written as

$$\begin{aligned} (f_1^i(X^i))^\omega &= \frac{(1 - r_s^i)^\omega + (r_s^i)^\omega \int (p_1^i(x))^\omega dx}{(1 - r_s^i)^\omega + (r_s^i)^\omega \int (p_1^i(x))^\omega dx} \\ &\times \begin{cases} (1 - r_s^i)^\omega & X = \emptyset \\ (r_s^i)^\omega p_{q,1}^i(x) \int (p_1^i(x))^\omega dx & X = \{x\} \\ 0 & \text{otherwise.} \end{cases} \\ &= \left[(1 - r_s^i)^\omega + (r_s^i)^\omega \int (p_1^i(x))^\omega dx \right] q_1^i(X). \end{aligned} \quad (80)$$

Substituting (78) and (80) into (7) results in (8) proving Lemma 1.

APPENDIX B

In this appendix we prove Theorem 2 on the product of PMBs. We can write (14) as

$$\begin{aligned} q(X) &\propto \sum_{X^0 \uplus \dots \uplus X^{n_1} = X} \left[q_1^p(X^0) \prod_{i=1}^{n_1} q_1^i(X^i) \right. \\ &\times \left. \sum_{Y^0 \uplus \dots \uplus Y^{n_2} = X^0 \uplus \dots \uplus X^{n_1}} q_2^p(Y^0) \prod_{j=1}^{n_2} q_2^j(Y^j) \right]. \end{aligned} \quad (81)$$

Let us focus on the inner sum. As Y^1, \dots, Y^{n_2} and $X^1 \dots X^{n_1}$ can have at maximum one element (otherwise the corresponding Bernoulli density is zero), we can assign the sets in Y^1, \dots, Y^{n_2} to the sets in $X^1 \dots X^{n_1}$. The sets in Y^1, \dots, Y^{n_2}

that remain unassigned will be associated with X^0 . The sets in $X^1 \dots X^{n_1}$ that remain unassigned will be associated to Y^0 . The sum can then be written as a sum over all possible assignments between Y^1, \dots, Y^{n_2} and $X^1 \dots X^{n_1}$, which we denote by the assignment set $\gamma \in \Gamma$, see the paragraph before Theorem 2 for its definition.

For the assignment $\gamma = \{\gamma_1, \dots, \gamma_n\}$, where $n \in \{1, \dots, \min(n_1, n_2)\}$ being $\gamma_i = (\gamma_i(1), \gamma_i(2))$, we have that

$$Y^{\gamma_i(2)} = X^{\gamma_i(1)}, \dots, Y^{\gamma_n(2)} = X^{\gamma_n(1)}. \quad (82)$$

In addition, for this γ , we denote the indices of the unassigned sets in X^1, \dots, X^{n_1} as $\{\gamma_1^{u,1}, \dots, \gamma_{n_1-n}^{u,1}\}$. Similarly, the unassigned sets in Y^1, \dots, Y^{n_2} have indices $\{\gamma_1^{u,2}, \dots, \gamma_{n_2-n}^{u,2}\}$. In the inner convolution sum in (81), there is the following equality

$$Y^0 \uplus Y^1 \uplus \dots \uplus Y^{n_2} = X^0 \uplus X^1 \uplus \dots \uplus X^{n_1}. \quad (83)$$

For the assignment γ using (82), this equality becomes

$$\begin{aligned} Y^0 \uplus X^{\gamma_1(1)} \uplus \dots \uplus X^{\gamma_n(1)} \uplus Y^{\gamma_1^{u,2}} \uplus \dots \uplus Y^{\gamma_{n_2-n}^{u,2}} \\ = X^0 \uplus X^{\gamma_1(1)} \uplus \dots \uplus X^{\gamma_n(1)} \uplus X^{\gamma_1^{u,1}} \uplus \dots \uplus X^{\gamma_{n_1-n}^{u,1}}. \end{aligned} \quad (84)$$

This implies that

$$Y^0 \uplus Y^{\gamma_1^{u,2}} \uplus \dots \uplus Y^{\gamma_{n_2-n}^{u,2}} = X^0 \uplus X^{\gamma_1^{u,1}} \uplus \dots \uplus X^{\gamma_{n_1-n}^{u,1}}$$

and

$$Y^0 = X^0 \uplus X^{\gamma_1^{u,1}} \uplus \dots \uplus X^{\gamma_{n_1-n}^{u,1}} \setminus \left(Y^{\gamma_1^{u,2}} \uplus \dots \uplus Y^{\gamma_{n_2-n}^{u,2}} \right). \quad (85)$$

We introduce an additional set U , representing objects that are unassigned in both densities, such that

$$X^0 = U \uplus Y^{\gamma_1^{u,2}} \uplus \dots \uplus Y^{\gamma_{n_2-n}^{u,2}} \quad (86)$$

and therefore (85) becomes

$$Y^0 = U \uplus X^{\gamma_1^{u,1}} \uplus \dots \uplus X^{\gamma_{n_1-n}^{u,1}}. \quad (87)$$

Summing over all assignment sets and substituting these results into (81) yields

$$\begin{aligned} q(X) &\propto \sum_{n=0}^{\min(n_1, n_2)} \sum_{\{\gamma_1, \dots, \gamma_n\} \in \Gamma} \sum_{Y^{\gamma_1^{u,2}} \uplus \dots \uplus Y^{\gamma_{n_2-n}^{u,2}} \uplus U \uplus X^1 \dots \uplus X^{n_1} = X} \\ &\times \prod_{i=1}^n q_1^{\gamma_i(1)} \left(X^{\gamma_i(1)} \right) q_2^{\gamma_i(2)} \left(X^{\gamma_i(1)} \right) \\ &\times q_2^p \left(U \uplus X^{\gamma_1^{u,1}} \uplus \dots \uplus X^{\gamma_{n_1-n}^{u,1}} \right) \prod_{i=1}^{n_1-n} q_1^{\gamma_i^{u,1}} \left(X^{\gamma_i^{u,1}} \right) \\ &\times q_1^p \left(U \uplus Y^{\gamma_1^{u,2}} \uplus \dots \uplus Y^{\gamma_{n_2-n}^{u,2}} \right) \prod_{i=1}^{n_2-n} q_2^{\gamma_i^{u,2}} \left(Y^{\gamma_i^{u,2}} \right) \end{aligned} \quad (88)$$

where the second line is the consequence of applying (82), the third line is the consequence of applying (87) and keeping

the unassigned Bernoulli components in density 1, the fourth line results from (86) and keeping the unassigned Bernoulli components in density 2.

Making use of the fact that

$$q_2^p \left(U \uplus X^{\gamma_1^{u,1}} \uplus \dots \uplus X^{\gamma_{n_1-n}^{u,1}} \right) \propto q_2^p(U) \prod_{i=1}^{n_1-n} q_2^p \left(X^{\gamma_i^{u,1}} \right)$$

$$q_1^p \left(U \uplus Y^{\gamma_1^{u,2}} \uplus \dots \uplus Y^{\gamma_{n_2-n}^{u,2}} \right) \propto q_1^p(U) \prod_{i=1}^{n_2-n} q_1^p \left(Y^{\gamma_i^{u,2}} \right),$$

we obtain

$$q(X) \propto \sum_{n=0}^{\min(n_1, n_2)} \sum_{\{\gamma_1, \dots, \gamma_n\} \in \Gamma} \sum_{U \uplus X^{\gamma_1(1)} \uplus \dots \uplus X^{\gamma_n(1)} \uplus Y^{\gamma_1^{u,2}} \uplus \dots \uplus Y^{\gamma_{n_2-n}^{u,2}} = X} \times \prod_{i=1}^n q_1^{\gamma_i(1)} \left(X^{\gamma_i(1)} \right) q_2^{\gamma_i(2)} \left(X^{\gamma_i(1)} \right) \times q_2^p(U) q_1^p(U) \times \prod_{i=1}^{n_1-n} \left[f_1^{\gamma_i^{u,1}} \left(X^{\gamma_i^{u,1}} \right) q_2^p \left(X^{\gamma_i^{u,1}} \right) \right] \times \prod_{i=1}^{n_2-n} \left[q_1^p \left(Y^{\gamma_i^{u,2}} \right) q_2^{\gamma_i^{u,2}} \left(Y^{\gamma_i^{u,2}} \right) \right]. \quad (89)$$

We can now write the previous expression as

$$q(X) \propto \sum_{n=0}^{\min(n_1, n_2)} \sum_{\{\gamma_1, \dots, \gamma_n\} \in \Gamma} \sum_{U \uplus W = X} q_2^p(U) q_1^p(U) \times \sum_{X^1 \uplus \dots \uplus X^{n_1} \uplus Y^{\gamma_1^{u,2}} \uplus \dots \uplus Y^{\gamma_{n_2-n}^{u,2}} = W} \times \prod_{i=1}^n q_1^{\gamma_i(1)} \left(X^{\gamma_i(1)} \right) q_2^{\gamma_i(2)} \left(X^{\gamma_i(1)} \right) \times \prod_{i=1}^{n_1-n} \left[q_1^{\gamma_i^{u,1}} \left(X^{\gamma_i^{u,1}} \right) q_2^p \left(X^{\gamma_i^{u,1}} \right) \right] \times \prod_{i=1}^{n_2-n} \left[q_1^p \left(Y^{\gamma_i^{u,2}} \right) q_2^{\gamma_i^{u,2}} \left(Y^{\gamma_i^{u,2}} \right) \right] \quad (90)$$

$$= \sum_{U \uplus W = X} q_1^p(U) q_2^p(U) \times \sum_{n=0}^{\min(n_1, n_2)} \sum_{\{\gamma_1, \dots, \gamma_n\} \in \Gamma} \sum_{X^1 \uplus \dots \uplus X^{n_1} \uplus Y^{\gamma_1^{u,2}} \uplus \dots \uplus Y^{\gamma_{n_2-n}^{u,2}} = W} \times \prod_{i=1}^n q_1^{\gamma_i(1)} \left(X^{\gamma_i(1)} \right) q_2^{\gamma_i(2)} \left(X^{\gamma_i(1)} \right) \times \prod_{i=1}^{n_1-n} \left[q_1^{\gamma_i^{u,1}} \left(X^{\gamma_i^{u,1}} \right) q_2^p \left(X^{\gamma_i^{u,1}} \right) \right]$$

$$\times \prod_{i=1}^{n_2-n} \left[q_1^p \left(Y^{\gamma_i^{u,2}} \right) q_2^{\gamma_i^{u,2}} \left(Y^{\gamma_i^{u,2}} \right) \right]. \quad (91)$$

Let us define

$$q^p(U) \propto q_1^p(U) q_2^p(U) \propto [\lambda_{q,1}]^U [\lambda_{q,2}]^U = [\lambda_{q,1} \cdot \lambda_{q,2}]^U \quad (92)$$

and

$$q_{i,j}(X) = \frac{q_1^i(X) q_2^j(X)}{\rho_{i,j}} \quad (93)$$

where

$$\rho_{i,j} = \int q_1^i(X) q_2^j(X) \delta X. \quad (94)$$

Then, the fused density can be written as

$$q(X) = \sum_{U \uplus W = X} q^p(U) q^{\text{mbm}}(W) \quad (95)$$

where $j \in \{1, \dots, n_2\}$

$$q^{\text{mbm}}(W) \propto \sum_{n=0}^{\min(n_1, n_2)} \sum_{\{\gamma_1, \dots, \gamma_n\} \in \Gamma} \sum_{X^1 \uplus \dots \uplus X^{n_1} \uplus Y^{\gamma_1^{u,2}} \uplus \dots \uplus Y^{\gamma_{n_2-n}^{u,2}} = W} \times \prod_{i=1}^n \rho_{\gamma_i(1), \gamma_i(2)} q_{\gamma_i(1), \gamma_i(2)} \left(X^{\gamma_i(1)} \right) \times \prod_{i=1}^{n_1-n} \left[\rho_{\gamma_i^{u,1}, 0} q_{\gamma_i^{u,1}, 0} \left(X^{\gamma_i^{u,1}} \right) \right] \times \prod_{i=1}^{n_2-n} \left[\rho_{0, \gamma_i^{u,2}} q_{0, \gamma_i^{u,2}} \left(Y^{\gamma_i^{u,2}} \right) \right]. \quad (96)$$

Then, the MBM density is

$$q^{\text{mbm}}(W) \propto \sum_{n=0}^{\min(n_1, n_2)} \sum_{\{\gamma_1, \dots, \gamma_n\} \in \Gamma} \left[\prod_{i=1}^n \rho_{\gamma_i(1), \gamma_i(2)} \right] \times \left[\prod_{i=1}^{n_1-n} \rho_{\gamma_i^{u,1}, 0} \right] \left[\prod_{i=1}^{n_2-n} \rho_{0, \gamma_i^{u,2}} \right] \times \sum_{X^1 \uplus \dots \uplus X^{n_1} \uplus Y^{\gamma_1^{u,2}} \uplus \dots \uplus Y^{\gamma_{n_2-n}^{u,2}} = W} \prod_{i=1}^n q_{\gamma_i(1), \gamma_i(2)} \left(X^{\gamma_i(1)} \right) \times \prod_{i=1}^{n_1-n} q_{\gamma_i^{u,1}, 0} \left(X^{\gamma_i^{u,1}} \right) \prod_{i=1}^{n_2-n} q_{0, \gamma_i^{u,2}} \left(Y^{\gamma_i^{u,2}} \right). \quad (97)$$

This density can also be written as

$$q^{\text{mbm}}(W) \propto \sum_{\gamma \in \Gamma} \left[\prod_{i=1}^{|\gamma|} \rho_{\gamma_i(1), \gamma_i(2)} \right] \left[\prod_{i=1}^{n_1-|\gamma|} \rho_{\gamma_i^{u,1}, 0} \right] \left[\prod_{i=1}^{n_2-|\gamma|} \rho_{0, \gamma_i^{u,2}} \right]$$

$$\begin{aligned}
& \times \sum_{X^1 \uplus \dots \uplus X^{n_1} \uplus Y^{\gamma_1^{u,2}} \uplus \dots \uplus Y^{\gamma_{n_2-|\gamma|}^{u,2}} = W} \prod_{i=1}^{|\gamma|} q_{\gamma_i(1), \gamma_i(2)} \left(X^{\gamma_i(1)} \right) \\
& \times \prod_{i=1}^{n_1-|\gamma|} q_{\gamma_i^{u,1}, 0} \left(X^{\gamma_i^{u,1}} \right) \prod_{i=1}^{n_2-|\gamma|} q_{0, \gamma_i^{u,2}} \left(Y^{\gamma_i^{u,2}} \right). \quad (98)
\end{aligned}$$

In the next subsection we calculate the Bernoulli-Bernoulli and Bernoulli-Poisson fused densities.

A. Calculation of fused densities

In this section, we calculate the Bernoulli-Bernoulli and Bernoulli-Poisson fused densities in (98).

1) *Bernoulli-Bernoulli densities*: The weight of a Bernoulli-Bernoulli fused density is

$$\begin{aligned}
\rho_{i,j} &= \int q_1^i(X) q_2^j(X) \delta X \\
&= (1 - r_{q,1}^i) (1 - r_{q,2}^j) + r_{q,1}^i r_{q,2}^j \int p_{q,1}^i(x) p_{q,2}^j(x) dx. \quad (99)
\end{aligned}$$

We then have that a fused Bernoulli-Bernoulli density is

$$q_{i,j}(X) = \begin{cases} r_{i,j} p_{i,j}(x) & X = \{x\} \\ 1 - r_{i,j} & X = \emptyset \\ 0 & \text{otherwise} \end{cases} \quad (100)$$

where

$$r_{i,j} = \frac{r_{q,1}^i r_{q,2}^j \langle p_{q,1}^i, p_{q,2}^j \rangle}{\rho_{i,j}} \quad (101)$$

$$p_{i,j}(x) = \frac{p_{q,1}^i(x) p_{q,2}^j(x)}{\langle p_{q,1}^i, p_{q,2}^j \rangle}. \quad (102)$$

2) *Bernoulli-Poisson densities*: The weight of a Bernoulli-Poisson fused density is

$$\begin{aligned}
\rho_{i,0} &= \int q_1^i(X) q_2^P(X) \delta X \\
&= 1 - r_{q,1}^i + r_{q,1}^i \langle p_{q,1}^i, \lambda_{q,2} \rangle. \quad (103)
\end{aligned}$$

Then, a Bernoulli-Poisson fused density is

$$q_{i,0}(X) = \frac{q_1^i(X) q_2^P(X)}{\rho_{i,0}} \quad (104)$$

where

$$q_{i,0}(X) = \begin{cases} r_{i,0} p_{i,0}(x) & X = \{x\} \\ 1 - r_{i,0} & X = \emptyset \end{cases} \quad (105)$$

and

$$r_{1,0} = \frac{r_{q,1}^i \langle p_{q,1}^i, \lambda_{q,2} \rangle}{\rho_{i,0}} \quad (106)$$

$$p_{i,0}(x) = \frac{p_{q,1}^i(x) \lambda_{q,2}(x)}{\langle p_{q,1}^i, \lambda_{q,2} \rangle}. \quad (107)$$

This completes the proof of Theorem 2.

APPENDIX C

In this appendix, we prove Lemma 5. We can write (45) as

$$\begin{aligned}
C[q] &= \omega \int q(X) \log \frac{q(X)}{f_1(X)} \delta X \\
&+ (1 - \omega) \int q(X) \log \frac{q(X)}{f_2(X)} \delta X \\
&= \int q(X) \log \frac{(q(X))^\omega}{(f_1(X))^\omega} \delta X \\
&+ \int q(X) \log \frac{(q(X))^{1-\omega}}{(f_2(X))^{1-\omega}} \delta X. \quad (108)
\end{aligned}$$

Now, we apply the upper bound (6) yielding

$$\begin{aligned}
& \log (f_1(X))^\omega \\
& \leq \log \sum_{X^0 \uplus \dots \uplus X^{n_1} = X} (f_1^P(X^0))^\omega \prod_{i=1}^{n_1} (f_1^i(X^i))^\omega. \quad (109)
\end{aligned}$$

We apply the similar upper bound to $\log (f_2(X))^{1-\omega}$, which results in the inequality

$$C[q] \geq L[q]$$

where

$$\begin{aligned}
L[q] &= \int q(X) \log \frac{(q(X))^\omega}{\alpha_1 q_1(X)} \delta X \\
&+ \int q(X) \log \frac{(q(X))^{1-\omega}}{\alpha_2 q_2(X)} \delta X \\
&= \int q(X) \log \frac{(q(X))^\omega (q(X))^{1-\omega}}{\alpha_1 q_1(X) \alpha_2 q_2(X)} \delta X \\
&= \int q(X) \log \frac{q(X)}{\alpha_1 q_1(X) \alpha_2 q_2(X)} \delta X \\
&= \int q(X) \log \frac{q(X)}{\frac{q_1(X) q_2(X)}{\langle q_1, q_2 \rangle}} \delta X - \log(\alpha_1 \alpha_2 \langle q_1, q_2 \rangle). \quad (110)
\end{aligned}$$

This completes the proof of Lemma 5.